Ultrastructure of the Connective Tissue Matrix

A. Ruggeri and P.M. Motta, editors

Martinus Nijhoff Publishers

Ultrastructure of the Connective Tissue Matrix

Edited by

A. RUGGERI, M.D.
Department of Anatomy, Faculty of Medicine
University of Bologna, Bologna, Italy

and

P.M. MOTTA, M.D., Ph.D.
Department of Anatomy, Faculty of Medicine
University of Rome, Rome, Italy

1984 **MARTINUS NIJHOFF PUBLISHERS**
a member of the KLUWER ACADEMIC PUBLISHERS GROUP
BOSTON / THE HAGUE / DORDRECHT / LANCASTER

Distributors

for the United States and Canada: Kluwer Boston, Inc., 190 Old Derby Street, Hingham, MA 02043, USA
for all other countries: Kluwer Academic Publishers Group, Distribution Center, P.O. Box 322, 3300 AH Dordrecht, The Netherlands

Library of Congress Cataloging in Publication Data

Main entry under title:

Ultrastructure of the connective tissue matrix.

(Electron microscopy in biology and medicine)
Includes index.
1. Connective tissues. 2. Ground substance (Anatomy) 3. Ultrastructure (Biology) I. Ruggeri, A. (Alessandro) II. Motta, Pietro. III. Series. [DNLM: 1. Connective tissue--Ultrastructure. 2. Collagen. 3. Proteoglycans. 4. Elastin. 5. Microscopy, Electron--Methods. QS 532.5.C7 U47]
QM563.U47 1984 611'.74 83-17326
ISBN 0-89838-600-4

ISBN 0-89838-600-4

Copyright

PRINTED IN THE NETHERLANDS

Ultrastructure of the connective tissue matrix

ELECTRON MICROSCOPY IN BIOLOGY AND MEDICINE

Current Topics in Ultrastructural Research

SERIES EDITOR: P.M. MOTTA

Already published in this series

Motta, P.M. (ed.): Ultrastructure of Endocrine Cells and Tissues.
ISBN: 0-89838-568-7.

Van Blerkom, J. and Motta, P.M. (eds.): Ultrastructure of Reproduction: Gametogenesis, Fertilization, and Embryogenesis. ISBN: 0-89838-572-5.

Preface

In recent years, the techniques of electron microscopy have developed so widely and rapidly that they now cover the fields of research once the unique apanage of sister research techniques such as biochemistry, physiology, immunology, X-ray diffraction, etc. It is now possible to reach molecular and submolecular levels, making this technique indispensable in every type of research. Electron microscopy alone often provides enough information to solve given problems.

In the field of the connective tissue matrix, knowledge of the molecular structure of collagen, proteoglycans and elastin and their interaction has been to a large extent elucidated by electron microscopy. The field over which electron microscopy ranges in the investigation of the connective tissue matrix is so wide that the aim of this volume is to collect the main ultrastructural acquisitions disseminated in various journals and monographs in one book.

The intent of this volume is to: (a) integrate different and new microscopic methods and review the results of such an integrative approach; (b) present a comprehensive ultrastructural account of selected aspects of the field; (c) point out gaps or controversial topics in our knowledge; (d) outline pertinent future research and expansion of the subject.

The chapters of this volume, prepared by recognized authorities in the field, briefly present traditional information on the topic, but mainly describe the very new trends on the subject, showing with the help of a rich and valuable selection of micrographs the contribution that these integrated submicroscopic techniques have produced in the field. It is hoped that this book will represent a valuable help to specialists concerned with the normal and pathological structure of the connective matrix in embryology, development, adult life and aging.

We wish to express our sincere thanks to the contributors of the volume and to all the members of the advisory scientific committee for having enthusiastically and patiently responded to our numerous requests during the preparation of the volume.

We also wish to carry out the desire of the contributors, and of the Italian Group for Calcified Tissue Research, in dedicating this volume to Prof. Rodolfo Amprino on his seventieth birthday. This dedication is an acknowledgement of his fundamental contribution to the study of bone development and of his constant and exemplary commitment in stimulating and coordinating research in the field of connective tissue.

Editors

List of contributors

Benazzo, Franco, Clinica Ortopedica, Università, 27100 Pavia, Italy

Bezerra, M.S.F., Laboratório de Biologia Celular, Faculdade de Medicina da USP, Av. Dr. Arnaldo 455, 01246 São Paulo, Brazil

Bonucci, Ermanno, Istituto di Anatomia Patologica, Policlinico Umberto I, Viale Regina Elena, 324, 00161 Roma, Italy

Chapman, John A., Department of Medical Biophysics, University of Manchester Medical School, Manchester M13 9PT, United Kingdom

Craig, Alan S., Applied Biochemistry Division, DSIR, Palmerston North, New Zealand

Fornieri, Claudio, Istituto di Patologia Generale, Via Campi, 287, 41100 Modena, Italy

Hulmes, David J.S., Department of Medical Biophysics, University of Manchester Medical School, Oxford Road, Manchester, M13 9PT, United Kingdom

Junqueira, Luiz C.U., Laboratório de Biologia Celular, Faculdade de Medicina da USP, Av. Dr. Arnaldo 455, 01246 São Paulo, Brazil

Kádár, Anna, 2nd Central Electron Microscope Laboratory, 2nd Department of Pathology, Semmelweis Medical University, Budapest IX., Üllöi-út 93, Hungary

Marchini, Maurizio, Istituto di Anatomia Umana Normale, Via Irnerio, 48, 40126 Bologna, Italy

Montes, Gregorio S., Laboratório de Biologia Celular, Faculdade de Medicina da USP, Av. Dr. Arnaldo 455, 01246 São Paulo, Brazil

Motta, Pietro M., Università di Roma, Istituto di Anatomia Umana Normale, Viale Regina Elena, 289, 00161 Roma, Italy

Parry, David A.D., Department of Chemistry, Biochemistry and Biophysics, Massey University, Palmerston North, New Zealand

Pasquali-Ronchetti, Ivonne, Istituto di Patologia Generale, Via Campi, 287, 41100 Modena, Italy

Reale, Enrico, Medizinische Hochschule Hannover, Abteilung Elektronenmikroskopie, Karl-Wiechert-Allee 9, D-3000 Hannover 61, Federal Republic of Germany

Ruggeri, Alessandro, Università di Bologna, Istituto di Anatomia Umana Normale, Via Irnerio, 48, 40126 Bologna, Italy

Serafini-Fracassini, Augusto, Department of Biochemistry and Microbiology, University of St. Andrews, St. Andrews, Fife KY16 9AL, United Kingdom

Thyberg, C. Johan O., Department of Histology, Karolinska Institutet, P.O. Box 60400, S-104 01 Stockholm, Sweden

Contents

CHAPTER 1

Electron microscopy of the collagen fibril

JOHN A. CHAPMAN and DAVID J.S. HULMES

1. Introduction

1.1. Identification of collagen

Collagen is identified by those properties that stem from the predominantly triple-chain helical structure of its molecules. A prerequisite for the formation of this triple helix is a Gly-X-Y repeating tripeptide unit in the amino acid sequence of the three chains, where X and Y can be any amino acids but are often the imino acids proline and hydroxyproline. This sequence, with glycine in every third position and with an unusual abundance of hydroxyproline, forms the basis for the chemical identification of collagen (for review, see 1). An unambiguous physical identification is provided by X-ray diffraction; the helix parameters established by high-angle X-ray scattering are unique to collagen (2).

Although electron microscopists have for many years identified collagen by its appearance as long unbranched banded fibrils with a characteristic periodicity of 60 – 70 nm (see, for example, Figures 3–8, it is now known that not all collagens exist in this form. Types I, II and III collagen all form periodic-structured fibrils, but type IV collagen molecules in basement membranes do not occur in the fibrillar form and aggregate instead as a mat-like network; less is known about the distribution and structure of other collagen types. Thus although characteristically banded fibrils are unmistakably collagen, this is not the sole criterion for the identification of mature collagen in the electron microscope.

Nevertheless, we shall be concerned here only with collagen in the fibrillar form and, in particular, with the molecular basis underlying its periodicity and the intraperiod band pattern. Type I collagen, the main constituent of tendon, skin, bone and vessel walls, has been studied for longer than other types, and more is known about its structure at all levels. It is the source of material for most of the experimental data presented in this chapter. The band patterns of type II and type III collagen fibrils differ only slightly from the type I pattern, implying a broadly similar axial arrangement of molecules in each of these fibril types.

1.2. The collagen molecule

A variety of physical and physiochemical studies, including direct visualisation of individual molecules in the electron microscope, have demonstrated the rod-like nature of the collagen molecule. Molecules of type I collagen have a length, L, which is slightly less than 300 nm and a diameter, 2r, of about 1.4 nm. The rod is neither rigid nor randomly flexible but appears to possess an intermediate level of semi-flexibility which probably varies along its length (3, 4). The three helically wound polypeptide chains ('α chains') which make up the rod each comprise about 1,000 amino acid residues. The details of the three-dimensional structure of the triple helix, established by X-ray diffraction and using known bond lengths and bond angles, have been reviewed elsewhere (2). For the interpretation of the intraperiod band pattern of the collagen fibril, we shall be less concerned with the structure in three dimensions than with the projection of that structure on to the molecular axis. From our point of view the parameter that matters is the residue-to-residue spacing, h, in an axial direction. This is known (from the position of the meridional reflection in the X-ray pattern) to be close to 0.29 nm (2). The known values for the D-periodicity (67 nm in rat tail tendon) and the number of residues in a D-period (= 234) show that the mean value of h is, more accurately, 0.286 nm. As the meridional reflection is diffuse, the assumption that the residues are uniformly spaced throughout the triple-helical body of the molecule is not strictly valid and the residue-to-residue spacing can be expected to vary slightly along the molecule.

Ruggeri, A and Motta, PM (eds): Ultrastructure of the connective tissue matrix. ISBN 0-89838-600-4.

1.3. Amino acid sequence

The three α-chains are non-identical in type I collagen, where the molecule comprises two identical α1(I) chains and one α2(I) chain, but are identical in type II and in type III. The amino acid sequences of the α1(I) and α2(I) chains are known (5); so too are the sequences of the α1(III) chain and most of the α1(II) chain. Species differences occur, but a substantial measure of homology between species exists. Of the 1,055 residues in the α1(I) chain of calf skin collagen, 1,014 occur in the repeating Gly-X-Y triplets essential for triple-helical packing. The N-terminal 16 residues and C-terminal 25 residues do not have glycine in every third position and exist in a less regular conformation. N-terminal and C-terminal extrahelical peptides occur at the ends of the 1,029-residue-long α2(I) chain but are shorter.

Some of these features are illustrated in Figure 1 which shows the amino acid sequences in the three α-chains at the N-end of a type I collagen molecule from calf skin. Roughly 5 per cent of a complete molecule appears in the figure. The N-terminal extrahelical peptides are on the left and the numbering of residues begins with the first glycine in the triple-helical part of the molecule. No attempt has been made to indicate the coiling of the chains. Although the residue-to-residue spacing, h, has been shown as constant throughout, this is far from being the case in the extrahelical peptides; their conformations, probably folded, are still in doubt. The formation of the triple helix requires the three chains to be mutually staggered by one residue to accommodate the glycines close to the central axis of the molecule and to allow the X and Y side-chains to project outwards. The position of the α2 chain with respect to the two α1 chains in type I collagen is not yet known with certainty; here the order α1–α2–α1 has been assumed. Throughout the sequences, the charged residues Arg, Lys, Asp, Glu are printed in bold capitals (this will later be used to mimic the effect of heavy metal staining); the residues His, Hyl, Glx (i.e. Glu or Gln), where the staining behaviour is less certain, are in small capital letters; all other residues are shown in italic. It will be noted that there is a marked tendency for charged residues to occur in groups (underlined), separated by stretches devoid of charge.

The complete sequence of type I collagen appears in Figure 13 a,b,c,d. About 80 per cent of the data are from calf skin; where calf skin data were not available, data from rat skin or (for the α2 chain only) chick skin have been used instead.

This knowledge of the amino acid sequences of the three α chains and the essentially one-dimensional nature of the collagen molecule, with its near-constant axial separation between residues in all but 3 per cent of its tertiary structure, now permit the direct correlation of structural data obtained by electron microscopy with chemical sequence data. In this respect collagen provides a valuable model system for studying the chemical basis of ultrastructure and the action of heavy metal stains and other reagents on a protein.

1.4. D-periodicity in fibrils

It has been recognised for some time that the periodic structure in collagen fibrils arises because the molecules are assembled in parallel array and are mutually staggered (i.e. axially displaced with respect to one another) by integral multiples of a common distance, D (6–9). Low-angle X-ray diffraction of hydrated, slightly stretched fibrils suggests that D is close to 67 nm in the native state in rat tail tendon collagen (10, 11), although the same technique has yielded slightly different values in other tissues, with the D-period in skin significantly shorter than in tendon (11–13). Electron microscopy, inevitably of dehydrated specimens, usually gives lower values, commonly around 64 nm in fibrils deposited on a supporting film from suspension. In embedded and sectioned material, values over a wide range can be encountered, presumably as a result of mechanical stresses imposed during sectioning.

The relative axial relationships between molecules in a fibril are illustrated in Figure 2. It is to be

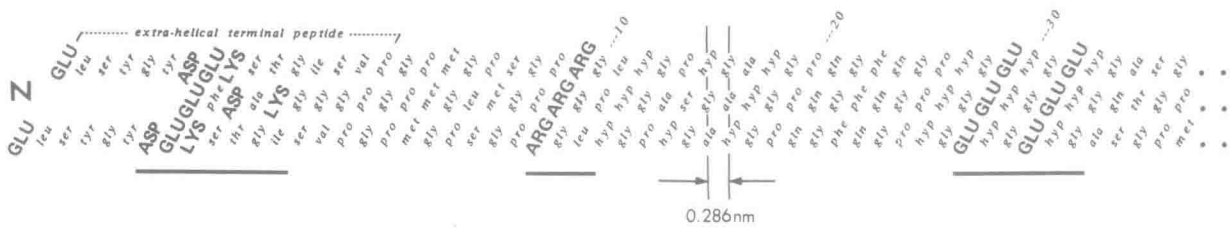

Figure 1. The triple-chain sequence of type I calf skin collagen at the N-end of the molecule. Bold capitals indicate charged residues.

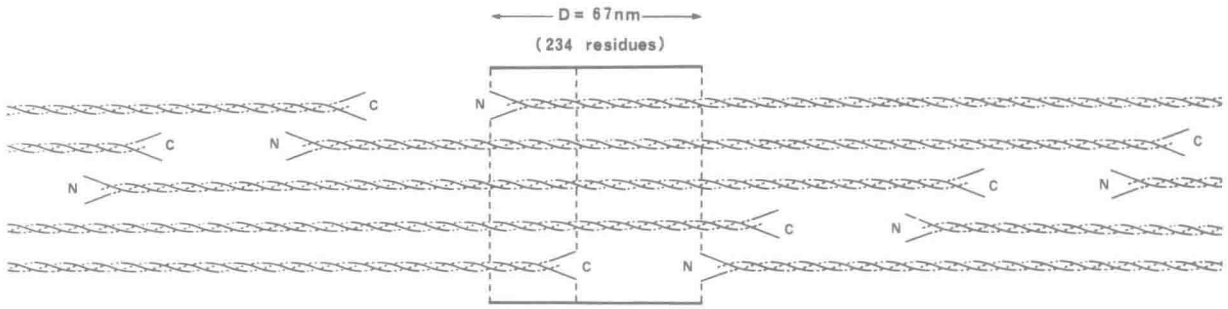

Figure 2. The regular staggering of molecules in a collagen fibril (the 'Hodge-Petruska' packing arrangement (9), first proposed by Tomlin (6)).

remembered that this is merely a diagrammatic representation in two dimensions and cannot show all possible stagger relationships in three dimensions (which could include not only the 1D and 4D staggered contacts shown here but also 0D, 2D and 3D staggers betwwen adjoining molecules). The figure shows, in essence, the predicted positions of molecules projected on to the fibril axis.

As the ratio of molecular length to D-stagger is non-integral (the values quoted here give L/D = 4.48), each D-period can be seen from Figure 2 to be divided into two roughly equal zones, an 'overlap' zone which includes the N- and C-ends of molecules, and a 'gap' zone which does not. For every five molecular segments in an overlap, there are only four in a gap zone, and the protein density in this zone can be expected to be roughly 4/5 that in the overlap zone. The ratio L/D = 4.48 implies that the axial extent of the overlap zone should be 0.48D but measurements on electron micrographs (see Section 3.5) indicate an axial extent closer to 0.40D. The difference is probably due to a condensed or folded conformation of the extrahelical terminal peptides in the dehydrated fibril, leading to a broadening of the gap.

2. The collagen fibril in the electron microscope

2.1. Selection and preparation

The earliest methods for the ultrastructural study of biological fibres involved dispersing or homogenising the tissue and depositing a small amount, suitably diluted, on a supporting film. This procedure is well suited to tendon (e.g. from rat tail) which is predominantly collagen but is less applicable to tissue in which extra-fibrillar material tends to obscure fibrils. The examination of intact tissues, with the aim of preserving the form of tissue components and the spatial relationships between them, came later with the development of embedding and ultrathin sectioning techniques. The adjoining chapter (14) is largely concerned with data obtained in this way. Newer techniques which permit the examination of surfaces (e.g. scanning electron microscopy, freeze-fracturing) are sometimes used as an alternative approach to the study of tissue components *in situ* (Chapter 4).

A further selective procedure applicable to collagen makes use of the property that collagen extracted from connective tissue (usually young) by weak acid or neutral salt solution can be made to reconstitute into native-type fibrils which exhibit an intraperiod band pattern indistinguishable from that in directly extracted native fibrils. As reconstituted fibrils can readily be prepared from purified solutions, yielding fibrils free of contaminants and with clearly defined staining patterns, they have been widely used for high-resolution studies of intraperiod structure. Most of the work described here, correlating staining patterns with amino acid sequence data, was carried out on reconstituted fibrils usually from citric acid or acetic acid extracted calf skin.

The reconstitution of fibrils from solution has received a good deal of attention, from physical chemists as well as electron microscopists. Although reconstitution *in vitro* superficially resembles growth *in vivo* it is now recognised that many other factors may operate *in vivo*. This has prompted fresh approaches to the selection of material for electron microscopic and other studies of fibril formation. As described later (Section 5.2), new information has emerged from the direct examination of macromolecular aggregates in the extracellular milieu around cultured fibroblasts actively synthesising collagen (15). More recently still, attempts have been made to prepare collagen fibrils from newly synthesised collagen precursor molecules (i.e. pro-

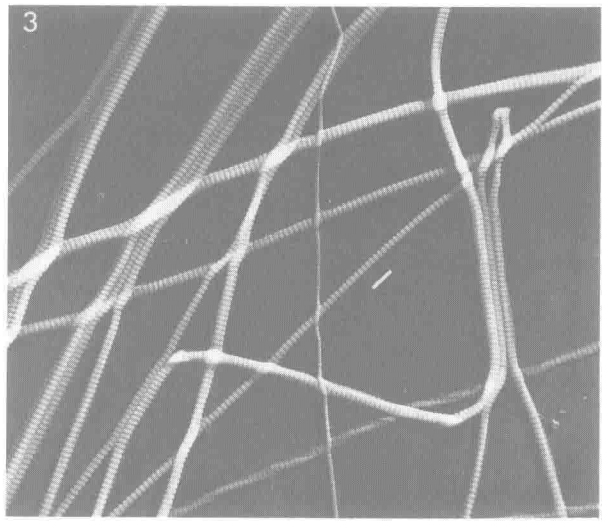
3

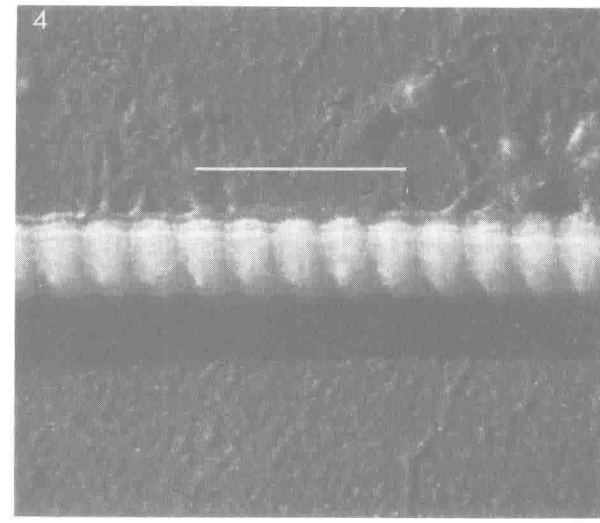
4

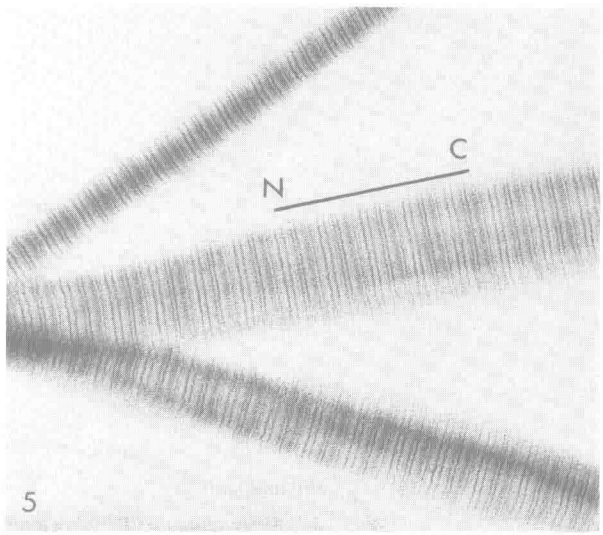
C
N
5

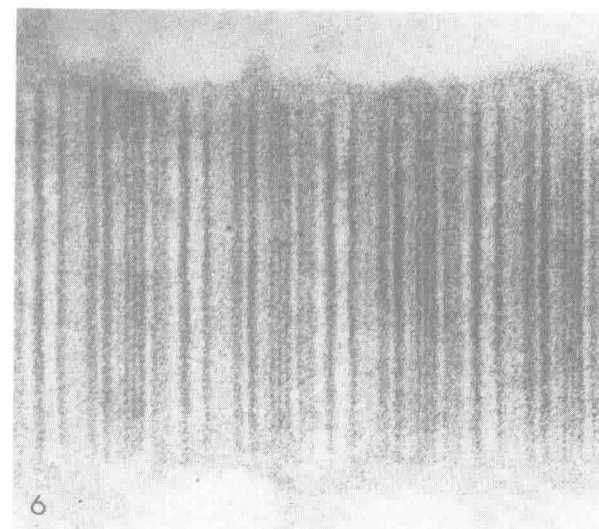
6

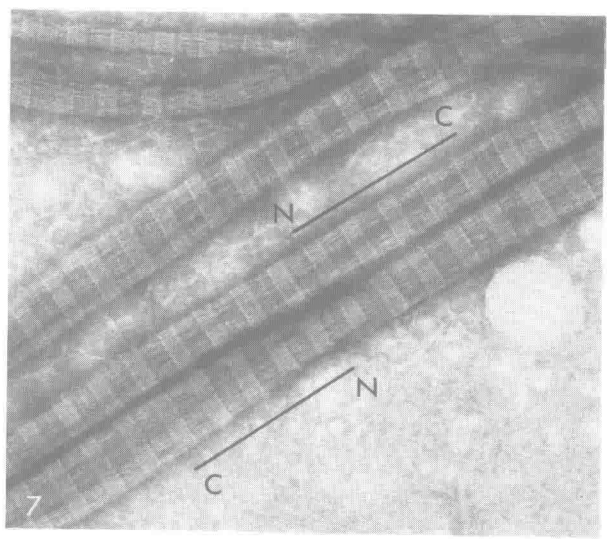
C
N
N
C
7

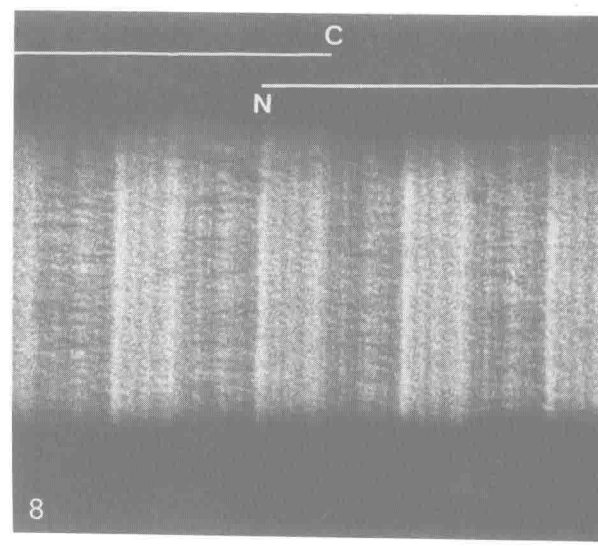
C
N
8

collagen) by enzymic removal of the propeptides *in vitro* (16).

2.2. *Enhancement of image constrast*

The elemental composition of most biological materials is such that the scattering of electrons differs little from one part of a specimen to another and contrast in the electron-optical image is therefore weak. There are various ways in which heavy metal atoms, which scatter electrons strongly, can be incorporated in the specimen to introduce contrast. Which of these contrasting methods has been used will influence markedly the appearance of a collagen fibril in the electron microscope.

In the early days of electron microscopy, shadowcasting was widely employed and gave useful information about the form of fibrils and their growth behaviour. Collagen fibrils, deposited from suspension on a supporting film and coated *in vacuo* with a thin layer of heavy metal at a small angle to the supporting film, display a striking 'gas mask tubing' appearance (Figures 3, 4). This appearance is, of course, due to the different mass thickness of the overlap and gap zones in the fibril and differential shrinkage after dehydration. The periodically changing surface contours of the fibril are accentuated by the shadow effect, particularly when the direction of evaporation of the heavy metal is other than at right angles to the fibril axis. In the conventional shadowcasting technique applied to objects as large as fibrils, resolution is limited to some tens of nm by aggregation effects in the evaporated metal layer and only rarely is it possible to detect any intraperiod surface substructure other than that arising from the gap-overlap mass distribution. Heavy metal shadowing can nevertheless be used to visualise individual collagen molecules deposited on a clean flat substrate (such as freshly cleaved mica); visualisation is improved by using rotary shadowing to coat the collagen molecules from all directions at a glancing angle.

The most extensively used contrasting technique in biological electron microscopy has always been staining with solutions of heavy metal salts. Indeed, it is the only technique normally applicable to sectioned material. The word 'staining' is used here to mean the procedure in which, after exposure of the specimen to the heavy metal salt solution, unreacted staining solution is removed by washing, leaving only those staining ions or molecules which have reacted specifically with the specimen (Figures 5, 6). We shall also refer to this procedure as 'positive staining' when there is possibility of confusion with the 'negative staining' technique (see below). Commonly used stains are uranyl and leads salts (so-called 'cationic stains') and salts in which the heavy metal is in the anion (e.g. phosphotungstate). A detailed interpretation of the image of the stain distribution in fibrils is considered in Section 3.

In negative staining (or 'negative contrasting') only excess heavy metal staining solution is drained off, and no attempt is made to remove unbound stain by washing. The result is to leave a thin layer of dried stain in and around the specimen, outlining it and filling internal voids with the electron-dense contrasting medium. The internal structure that can be revealed depends on the size of the heavy metal staining molecule and the extent to which it can penetrate. In collagen fibrils the interstices in the gap zones are large enough to be readily penetrable, giving the characteristic alternation of dark (gap) and light (overlap) zones along the negatively stained fibrils (Figures 7, 8). Oddly, one of the first electron micrographs of a negatively stained fibril to be published (18) appeared before the technique itself was recognised and described. Several years elapsed before the technique was intentionally applied to collagen (19, 20).

2.3. *Positive and negative staining patterns*

When collagen fibrils are exposed to solutions of heavy metal salts, up to twelve staining bands per period can be distinguished (21). Band patterns in positively stained fibrils appear in Figures 5, 6, 10b. The asymmetric nature of the pattern (i.e. absence of mirror symmetry) implies a polarisation in direction of the molecular units in the fibril. The labelling of the bands in a D-period, shown in Figure 9a, follows the conventional notation in which groups of bands are denoted by letters and each band within a

←

Figures 3, 4. Collagen fibrils from human Achilles tendon, shadowed with gold-palladium. The periodicity is ~65 nm. The line represents the length of a collagen molecule (~300 nm).

Figures 5, 6. Calf skin collagen fibrils reconstituted from solution, positively stained with phosphotungstic acid (PTA) and uranyl acetate (UA). The periodicity is ~65 nm. In Figure 5, the line shows the length and polarity of a collagen molecule.

Figures 7, 8. Negatively stained calf skin collagen fibrils (Figure 7: PTA; Figure 8: lithium tungstate). The periodicity is ~65 nm. The lines indicate collagen molecules.

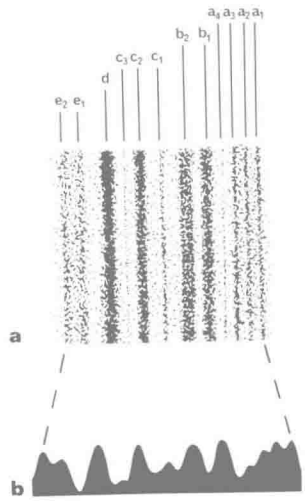

Figure 9. Labelling of the bands in a single D-period of a positively stained fibril (Figure 9a), and, below, a microdensitometric trace of the stain distribution (Figure 9b).

group is distinguished by a numerical suffix. An alternative, wholly numerical, notation has been proposed (22) but has not found wide acceptance, probably because the old notation is too well established. The four closely spaced **a** bands in the pattern have a mean centre-to-centre spacing of 3.4 nm and provide a useful test of pattern resolution. All staining patterns here are shown with the collagen molecules directed so that their N-ends point to the left (which results in a reversed alphabetical order for the lettering of the bands).

The pattern is readily observable in stained sections of embedded connective tissues in regions where collagen fibrils are sectioned longitudinally, although the section thickness is usually sufficient to reduce specimen resolution in the image to a level where the four **a** bands cannot be distinguished. As noted earlier (Section 2.1) the most clearly resolved band patterns are obtainable from reconstituted fibrils (Figure 10b). This is probably because fibrils prepared by reconstitution *in vitro* are less compact than those formed *in vivo* and flatten on the supporting film on drying, giving thinner specimens in which higher resolutions are attainable; distortion is often present, however, and fields of view with such clearly defined bands as those in Figure 10b are infrequent. It is not unusual to observe a slight curving of the bands, as in Figures 17 and 18; there is a marked tendency for this to be greatest in band $\mathbf{c}_2$ and for the curvature to be directed with its concave side to the right (i.e. in the N→C direction). It is most readily seen in micrographs by observing the pattern at a glancing angle. The frequent occurrence of this effect suggests that it is not a random distortion but reflects a basis structural feature in the fibril. As the N-ends of molecules terminate at the $\mathbf{c}_2$ band, the implication is that these N-ends are under tensile strain. This strain cannot be uniform across the fibril but must be greatest in its peripheral regions.

The D- staggered arrangement of molecules in a fibril was first elucidated by comparing positive staining patterns from fibrils with those from segment long spacing (SLS) collagen. Superposition of four SLS patterns, mutually staggered by D, was shown to give a pattern resembling that from a fibril (7,23). At the time it was thought that the molecular length, L, was 4D and the proposed molecular array was therefore referred to as 'quarter-staggered'.

The negative staining pattern, by locating the positions of the ends of the molecules, gives a more complete picture. The conspicuous subdivision of each D-period into a stain excluding (overlap) zone and a stain-accessible (gap) zone reveals the non-integral relationship between L and D in which L is approximately 4.4D (9). Figure 10a, b shows the negative and positive staining patterns compared; the D-staggered molecular array is indicated above. It is evident from this figure that the N-end of the molecule (at the left margin of each overlap zone) lies in the vicinity of the $\mathbf{c}_2$ band in a fibril and that the C-end occurs close to the $\mathbf{a}_3$ band.

The pattern from a negatively stained fibril appears to have a dual character. Although the principal contrast effects come from the gap-overlap subdivision of each D-period, superimposed on this pattern of broad light and dark zones is a finer band pattern similar to that obtained after positive staining. As suggested by others (9, 24) negative staining patterns would seem to retain an element of positive staining as well (see also Section 3.4).

3. The chemical basis of the staining pattern

3.1. Introduction

In the image of any stained biological specimen, the electron microscopist is viewing the products of a chemical reaction. Knowledge of the nature and extent of this reaction and of the factors that influence it should lead to a greater understanding of the significance of the image. As soluble reactants and products are removed in the positive staining procedure, only products bound to the specimen will contribute to the image. In positive staining, therefore, the important question is: what are the chemical groups on the specimen involved in this binding reaction?

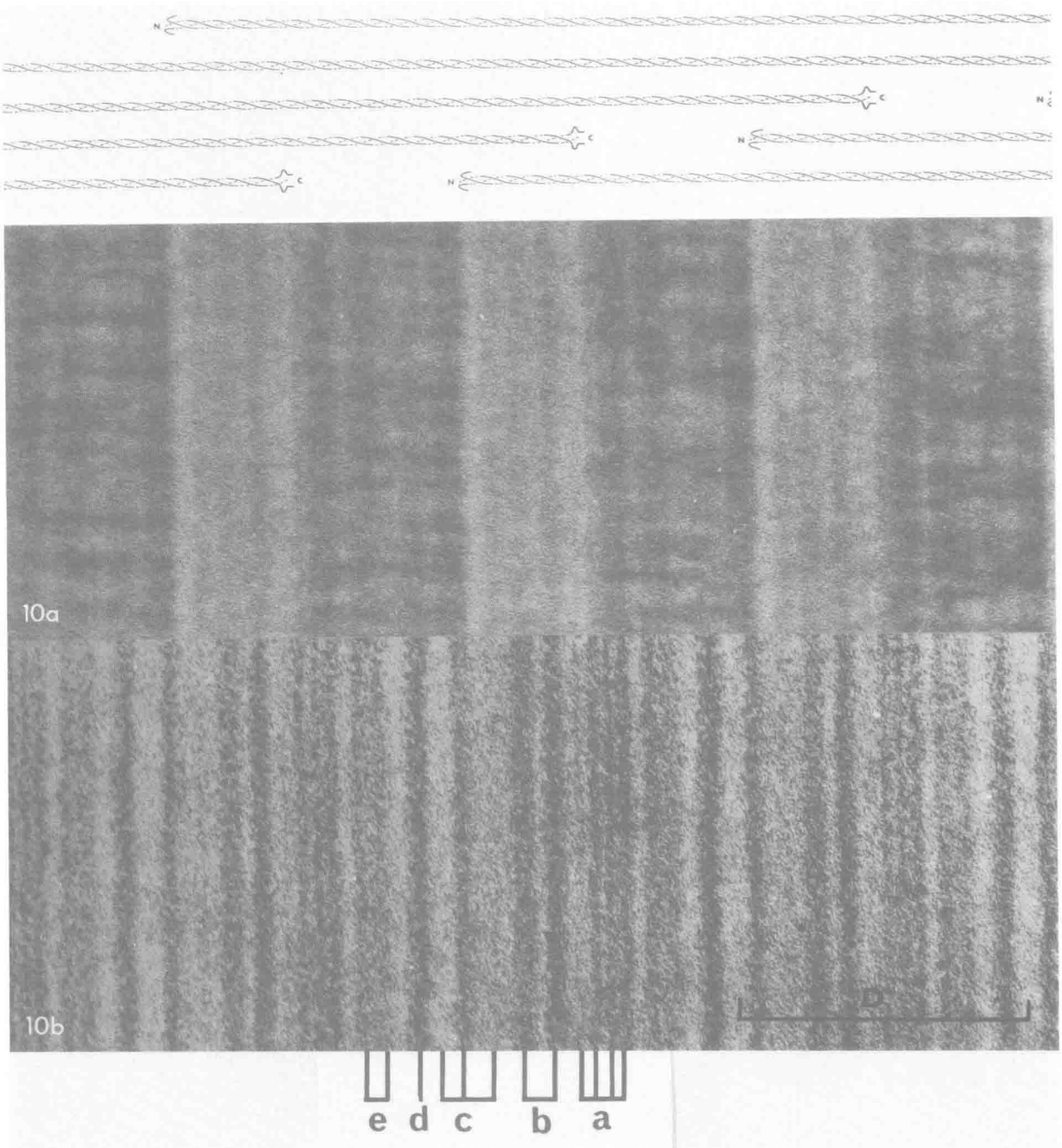

Figure 10. Matching of the negative staining pattern (Figure 10a) with the positive staining pattern (Figure 10b). The corresponding array of D-staggered molecules appears above, suitably aligned.

The characteristic band pattern exhibited by collagen stained with heavy metal salts has long been thought to be due to the uptake of the heavy metal ions on charged amino acid side groups along the collagen molecules (7,8). With current knowledge of the amino acid sequences of the polypeptide chains of collagen, this is most clearly demonstrated by a direct comparison of the band pattern from stained SLS collagen with the molecular charge distribution predicted by the sequence data (see Section 4.1 and Figure 11a, b). For type I collagen the molecular charge distribution is the summation of two α1

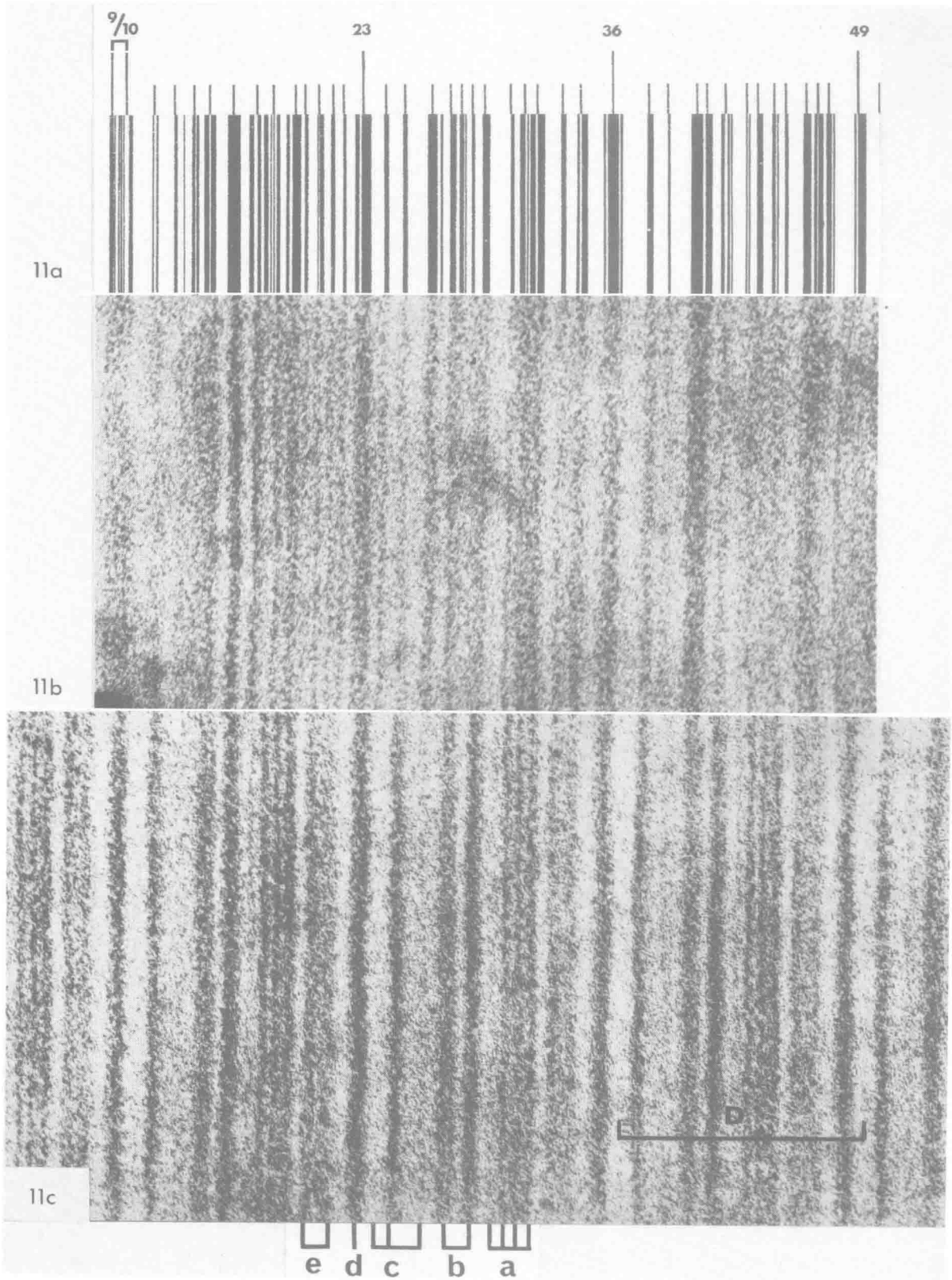
9/10
23
36
49
11a
11b
11c
D
e
d
c
b
a

charge distributions and one α2 charge distribution. The substantial measure of agreement between the location of charged residues in the summed 2α1 + α2 charge distribution and the location of dark bands in the SLS staining pattern means that this pattern can legitimately be described as the 'molecular staining pattern' (21) It is also evident that discrete staining bands exist because the charged amino acid residues tend to occur in groups, separated by regions sparsely populated with charged residues.

3.2. Comparison of the fibril staining pattern with sequence data

The relationship between the fibril staining pattern and the SLS-derived molecular pattern, first established in 1960 in the classic studies of Hodge and Schmitt (7) and Kühn et al. (23) and extended three years later by Hodge and Petruska (9) into the 'gap-overlap model' of axial molecular packing (Figure 2), can also be viewed in the light of the chemical sequence data. We note first, from Figure 11b, c, that the bands in the aperiodic SLS pattern can, for the most part, be matched in position, although not in intensity, with bands in the periodic fibril pattern. This result shows that a considerable measure of charge–charge association must occur when collagen molecules assemble into fibrils; equally, apolar regions sparse in charge will tend to associate with other apolar regions.

An essential step in the interpretation of the fibril staining patterns in terms of sequence data is the accurate determination of the relative axial positioning of the assembled molecules. We need to know how an amino acid residue on one molecule is positioned with respect to amino acid residues on neighbouring staggered molecules. This requires a precise evaluation of D in terms of residue spacings. An accuracy rather better than one residue spacing is called for, bearing in mind that an error of one residue in D will lead to a mismatching of four residue spacings between molecules in 4D-staggered contact. The accuracy with which h, the axial residue-to-residue spacing, can be established by X-ray diffraction is only sufficient to establish the number of residue spacings in D to within 2 – 3 spacings (i.e. D must be in the range 231 – 236 residue spacings)

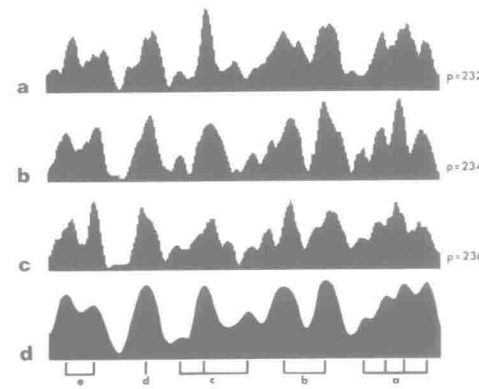

Figure 12. Predicted charge distributions in the fibril, assuming that the number of residues in a D-period is 232, 234, 236 (Figure 12a, 12b, 12c). Distributions are based on α1 and α2 sequence data and have been 'smoothed' to assist comparison with the observed fibril staining pattern. Highest correlation with the stain intensity distribution (Figure 12d) occurs when a D-period comprises 234 residue spacings.

D can be found with greater accuracy than this by comparing the fibril staining pattern with the pattern predicted by the sequence. This is done for a range of values of D, seeking that value which gives best agreement. Figure 9b shows the distribution of stain intensity in a single D-period of doubly stained collagen. This intensity distribution was obtained by microdensitometry of patterns such as that shown in Figure 10b. The axial distribution of charge in a D-period (for a chosen value of D) can be predicted from sequence data by summing five D-staggered molecular charge distributions (four in the gap zone). The result of this summation is shown in Figure 12a,b,c for D equal to 232, 234 and 236 residue spacings respectively. To assist comparison with the staining pattern, in which image resolution is unlikely to be better than 2.5 nm, the predicted charge distributions have in each case been 'smoothed' by 7 residue spacings (i.e. convolved with a smoothing function of this width). Below, in Figure 12d, appears the stain intensity distribution of Figure 9b for comparison with the smoothed charge distribution. This comparison, particularly in the region of the four closely spaced **a** bands, suggests that agreement is best when D is equal to 234 residue

←

Figure 11. The black lines in Figure 11a show the locations of charged residues in the central part of a type I collagen molecule, as predicted by α1 and α2 sequence data. Figure 11b is the band pattern from SLS collagen (stained with PTA and UA), matched with the charge distribution over this central region. (A comparison covering the whole molecule appears in Figure 22.) Figure 11c is the fibril staining pattern, aligned with the SLS pattern and showing how SLS and fibril bands match in position but not intensity. The numbering of the SLS bands is indicated above Figure 11a; bands 9/10, 23, 36, 49 are those contributing to the **d** line in the fibril.